Addressing Global Water Stress Using Desalination and Atmospheric Water Harvesting: A Thermodynamic and Technoeconomic Perspective

Jordan D. Kocher and Akanksha K. Menon[*]

George W. Woodruff School of Mechanical Engineering, Georgia Institute of Technology, Atlanta, GA, USA

*Corresponding author. Email: akanksha.menon@me.gatech.edu

Abstract

Freshwater is a critical resource for many sectors of the economy, but excessive withdrawal of natural freshwater reserves has resulted in global water stress that is projected to impact 4 billion people by the end of this decade. Methods of artificially producing freshwater include desalination, which is a well-established technology in which water is extracted from a saline solution (typically seawater). Atmospheric water harvesting (AWH) is an alternate emerging approach in which water vapor is extracted from ambient air and condensed into freshwater. AWH has recently attracted attention for decentralized water production, but a comparative analysis of these different technologies using the same performance (kWh/m^3) and cost metrics ($/m^3) does not exist. Herein we develop the first thermodynamic and technoeconomic framework for clean water production that considers the population and water risk across all global locations. We find that AWH consumes more energy than practical desalination with subsequent water transport for roughly 90% of the global population, even when AWH operates under reversible (albeit impractical) operation. Furthermore, a practical AWH system is far more expensive (6× − 40× depending on the location and AWH technology used) than seawater desalination on a levelized cost of water

(LCOW) basis, even after accounting for the costs associated with transporting desalinated water inland. The one exception is when water transport costs are increased by 5×, resulting in sorbent AWH becoming the lowest cost option for arid locations far from the coast (*e.g.,* Sahara Desert). Our analysis framework informs cost and performance targets (material and system level design tradeoffs) for technology deployment that maximizes global impact.

Introduction

The increasing demand for clean water has resulted in global water crises[1,2], with over 2 billion people experiencing water stress according to UN Water[3]. Climate change, population growth, and economic activities (agriculture, power generation, etc.) have exacerbated water scarcity by depleting natural freshwater reserves[2,4], thus necessitating the use of cost-effective methods for artificially producing clean water. Seawater desalination[5,6] is a well-established technology for separating salts from water that has been deployed in many coastal locations – for example, most of the Gulf countries satisfy nearly (or in some cases more than) 100% of their water demand for potable consumption using large desalination plants[7]. However, over 60% of the global population is located in inland regions (more than 100 km from the coast)[8], which has led to the emergence of distributed desalination[9]. One such distributed method involves seawater desalination at the coast followed by transportation of this clean water inland[10]. Desalination of inland saline water (*e.g.,* brackish groundwater, industrial wastewater, brines, etc.[11–14]) is another option for distributed freshwater production[9,15]; however, its applicability is determined by the availability of inland saline water sources which can be geographically widespread and of varying salinity.

Atmospheric water harvesting[16–24] (AWH) is another method of producing freshwater, and it has recently received great interest as an alternative to desalination, although no largescale systems have been demonstrated. In AWH systems, water vapor is extracted from ambient air and condensed into liquid water. Thermodynamically, desalination and AWH perform the same fundamental process, in that they both separate water from a mixture (salt/water for desalination and air/water for AWH) as show in Fig. 1a. The difference lies in the water activity of saltwater vs. humid air which determines the energy required to separate water from a mixture; an aqueous mixture with a lower water activity requires more energy to extract pure water. The water content in ambient air is much more dilute than in seawater, making AWH more energy intensive than seawater desalination – the median global water activity of atmospheric air (*i.e.*, relative humidity) is 0.65, whereas the activity of seawater is 0.97.

Recently there have been efforts to quantify the thermodynamic limits of AWH given its appeal as a means for producing freshwater using different approaches. Rao *et al.* evaluated the least work of separation for AWH and compared it to the thermodynamic performance of partially idealized AWH systems (such as a Carnot refrigerator that is internally reversible but harvests water via condensation which is irreversible) to determine which system is most energy efficient under different ambient conditions[17]. Kwan *et al.* also analyzed the least work of separation and quantified how much more energy is consumed by various practical desalination and AWH systems reported in the literature compared to the reversible limit[25]. LaPotin *et al.* developed a two-stage sorbent-based AWH device that could produce 0.77 L/m^2/day[24], and Li *et al.* developed a thermodynamic model of the performance of single and multi-stage sorbent AWH systems[26]. Researchers have also quantified the potential of AWH to meet water needs around the globe. For

example, Lord *et al.* used global irradiance data to estimate the water production from solar-driven AWH and found that it could provide drinking water to a billion people[22].

However, there is no direct comparison between AWH and desalination on the basis of their specific energy consumption (kWh/m^3). This is the first aim of our work: to analyze and compare the energy consumption of desalination and AWH using global weather data (NASA's MERRA 2 grid of temperature and humidity data[27]). We also normalize these results by the population, as well as the product of the population and water risk to understand how these systems would perform in locations where they would be most needed, which has not been reported thus far. Furthermore, the costs associated with such systems on a levelized basis (in $\$/m^3$) is lacking, despite the fact that AWH is often reported as being "low cost"[22,24,26]. For example, Siegel and Conser estimated the LCOW of sorbent-based AWH systems in Southern California[28], but they made no comparison to the cost of desalination or costs in other locations. This is the second aim of our work: to evaluate the LCOW of different AWH technologies across the globe and compare it to coastal seawater desalination with costs added to transport the clean water to different locations inland (using MATLAB's built-in Global Self-Consistent Hierarchical High-Resolution Geography data, and vertical and horizontal water transportation costs data[10]), as shown in Fig. 1b. We analyze three different AWH technologies: moisture condensation using vapor compression (dewing from active cooling)[29], condensation using radiative cooling surfaces (dewing from passive cooling)[30], and heat-driven sorption systems (desiccants)[19,26] for moisture capture as shown in Fig. 1c. We determine the LCOW of practical (irreversible) AWH systems as well as hypothetical reversible AWH systems, to find the lowest LCOW that they can achieve by improving energy efficiency alone. For the practical systems we focus on three representative

locations that span the range of climates: Aruba (very humid), Niger (very dry), and Perth (highly variable humidity). For the reversible systems, we calculate the LCOW in all global locations.
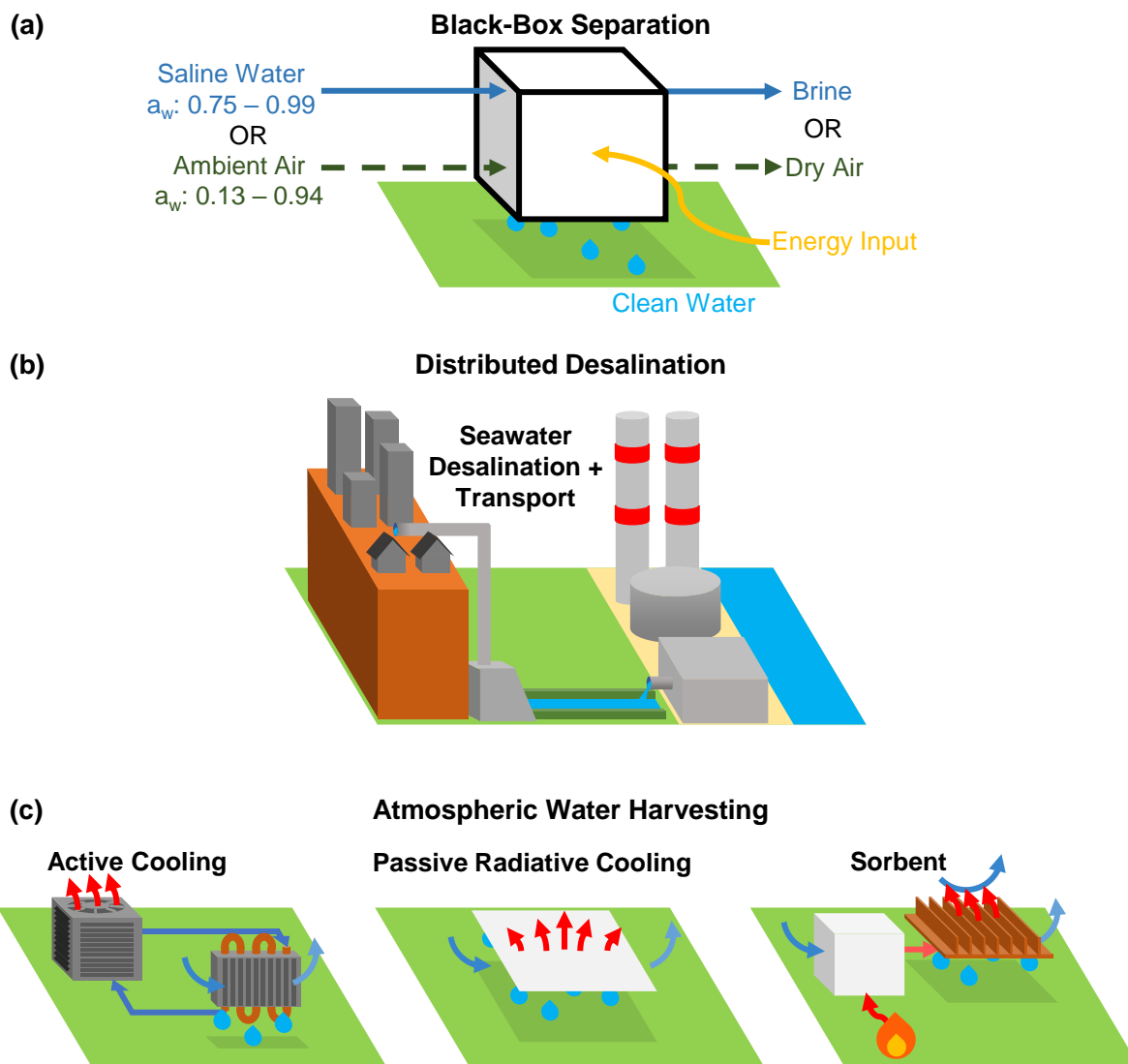
(a)

Black-Box Separation

Saline Water
a_w: 0.75 – 0.99

OR

Ambient Air
a_w: 0.13 – 0.94

Brine

OR

Dry Air

Energy Input

Clean Water

(b)

Distributed Desalination

Seawater Desalination + Transport

(c)

Atmospheric Water Harvesting

Active Cooling

Passive Radiative Cooling

Sorbent

Fig. 1 | Desalination and AWH technologies analyzed in this work. a. Black-box separator, where water enters as a mixture (saline water or humid air) and clean water is extracted using some energy input. **b.** The distributed desalination approach: seawater desalination at the coast uses reverse osmosis (RO) to produce clean water that is transported inland using pipes, canals, and tunnels. **c.** Three different atmospheric water harvesting technologies are considered: active cooling (a vapor compression air conditioner cools the air below the dew point to condense water), passive radiative cooling (surface rejects heat to outer space and cools the air below the dew point to condense water), and sorbent systems that desorb moisture (when heat is applied) at a higher dew point than the ambient and then cool this humidified air to ambient to condense moisture.

Thermodynamic framework for energy consumption

To compare the thermodynamic limits of AWH and desalination, we first derive the least work of separation, W_{min}, as a function of water activity in Eq. (1), which applies to any internally and externally reversible system that produces pure water (Fig. 1a).

$$W_{min} = -R_w T_{amb} \ln(a_w) \tag{1}$$

where R_w is the specific gas constant of water, T_{amb} is the ambient temperature (K), and a_w is the water activity. For humid air, a_w is equivalent to the relative humidity. For saline water, a_w is equal to the product of the mole fraction of water and the activity coefficient. When the mole fraction of water is high (~0.97 in seawater), the activity coefficient is nearly unity, and the activity of saline water approaches the water mole fraction.

Eq. (1) applies to reversible work-driven separation, while the energy required for reversible heat-driven separation is equal to the reversible work (Eq. (1)) multiplied by a factor of $\left(1 - \frac{T_{amb}}{T_s}\right)^{-1}$, where T_s is the heat source temperature. In Fig. 2a, we plot the least work of separation as a function of water activity (the solid black curve) and indicate the ranges of water activities corresponding to ambient air and saline water (ranging from brackish water at a salinity of 8.15 g/kg to saturated brine at 360 g/kg). Dashed lines indicate the median value of the annual average relative humidity experienced by the global population and the global water risk weighted population (Methods). This reveals that 50% of the population is located in regions where the average annual relative humidity is lower than 68% (activity <0.68). Meanwhile, the activity of seawater is ~0.97; this confirms that AWH inherently consumes more energy than desalination, by over an order of magnitude (~0.8 kWh/m³ for desalination and ~20 kWh/m³ for AWH under

reversible operation). For simplicity, we consider only work-driven separation in this section; a comparison on the basis of heat input is shown in Supplementary Note 4.
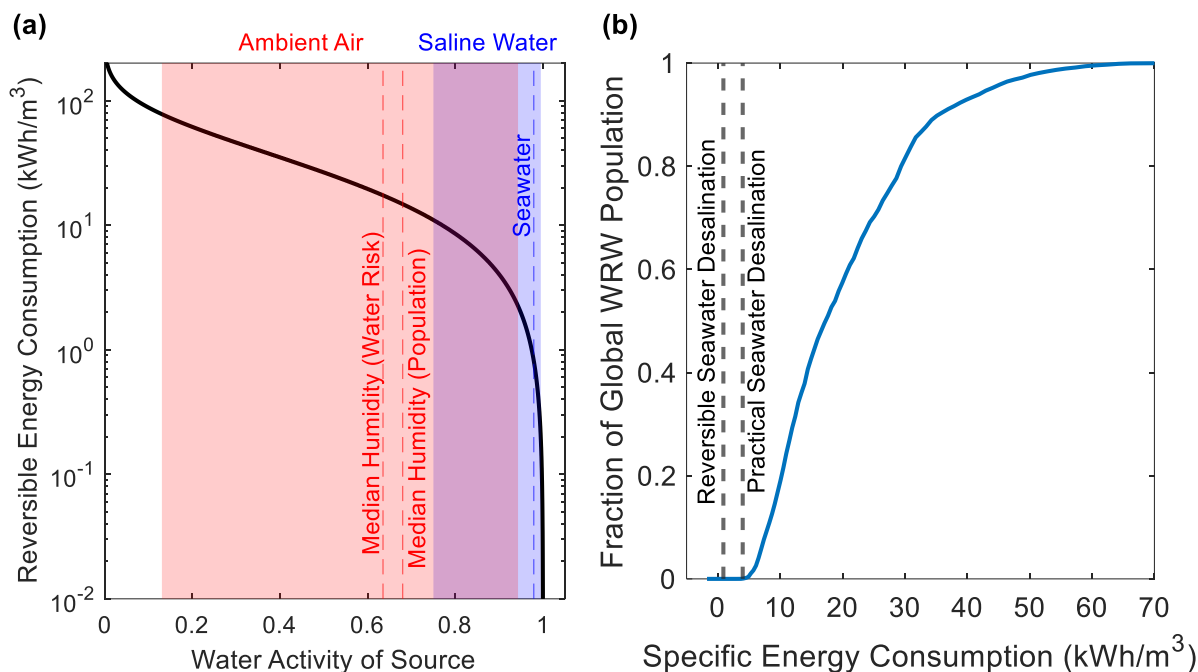

Fig. 2 | Thermodynamic limits of water separation. a. The reversible specific energy consumption of AWH and desalination as a function of water activity. The global population weighted median relative humidity is approximately 68%, while the global water risk weighted median relative humidity is 63.5%. The water risk weighting factor is the product of water risk and population within each grid cell (weather, population, and water risk datasets are references in Methods). **b.** Cumulative distribution plot showing the fraction of the water risk weighted (WRW) global population that lives in a location where the reversible specific energy consumption (SEC) of AWH would be below a certain value. Vertical dashed lines are given for the reversible and practical SEC values for seawater desalination with a salinity of 35 g/kg.

Next, we plot a cumulative distribution of global reversible AWH (solid blue curve), which represents the fraction of the global water risk weighted (WRW) population with access to reversible AWH at an energy consumption below a certain value. In Fig. 2b, we compare this to the energy consumption of both reversible and practical (using reverse osmosis) seawater desalination (dashed lines); refer to Supplementary Note 1 for details. We find that 0% of the population lives in a region where reversible AWH would be more energy efficient than reversible or practical seawater desalination using reverse osmosis. This suggests that if seawater (or any other saline water source with a lower salinity, *e.g.*, brackish groundwater) is locally available,

desalination is always more energy efficient than AWH. We note that practical AWH is not considered because these systems often require phase change of water, resulting in a much higher energy consumption (the latent heat of vaporization/condensation is 667 kWh_{th}/m^3).

While seawater desalination is efficient, it is not readily available at locations away from the coast. To meet clean water demands in this scenario, desalinated water from the nearest coast can be transported inland using some pumping energy (see Supplementary Note 3). AWH on the other hand can be implemented at any location for freshwater production. To evaluate which option is viable, we compare the reversible energy consumption of AWH to the practical energy consumption of seawater desalination with transport. We find that a practical (irreversible) seawater desalination system with transport of the clean water inland is still more energy efficient in most global locations, as shown in Fig. 3a. To enable a direct comparison, we also plot the fraction of global land area where either the desalination or AWH technology would be the most energy efficient (*i.e.*, the fraction of the map that is filled with the corresponding color in Fig. 3a) – this is shown as the "Area Weighted" results in Fig. 3b. The "Population Weighted" results and the "Water Risk Weighted" results represent the fraction of global population and global WRW population, respectively, for whom either technology would be most efficient. Notably, reversible AWH would be the most efficient option for roughly 40% of global locations, as shown by the large red region in Fig. 3a. However, when the population density or water risk weighting factors are considered, we find that AWH systems, even if they were engineered to be thermodynamically reversible, would only be more efficient than practical seawater desalination with transport for roughly 15% of the global WRW population. We note that Fig. 3 assumes that desalination, water transport, and AWH are all work-driven. However, sorbent-based AWH is typically heat-driven –

we find that even in this case the overall trends remain unchanged, with reversible sorbent AWH being more efficient for 15-20% of the global WRW population (Supplementary Note 4).
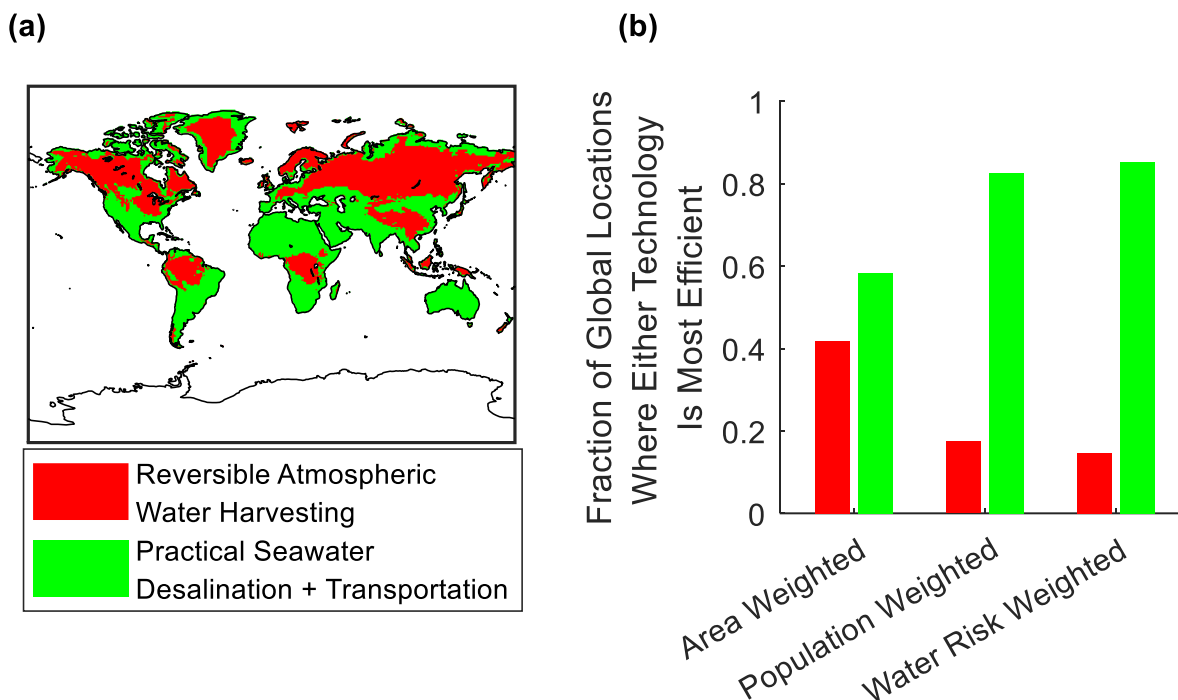
(a)   **(b)**

Fig. 3 | Reversible atmospheric water harvesting vs. practical distributed desalination. a. Map of the global land area (excluding Antarctica) shaded by the technology that would be more energy efficient: reversible atmospheric water harvesting or practical seawater desalination with transport of clean water inland. **b.** Fraction of the global land area where each technology would be more energy efficient. Results are presented where each grid cell is either weighted by area, weighted by the population within the cell, or weighted by the product of population and water risk within the cell.

Overall, this thermodynamic analysis and comparison with existing desalination systems conclusively shows that AWH is inherently more energy intensive for freshwater production across the globe even when reversible operation (albeit impractical) is assumed. However, a thermodynamic comparison alone is not sufficient for technology selection since cost is a major driver. In other words, AWH could be advantageous from a cost standpoint given that it is not infrastructure-heavy like desalination even though it is not suitable from an energetic standpoint – this is the focus of the next section.

Technoeconomic modeling framework for water cost

Given the lack of specific cost ($/m³) data for AWH, we first calculate the cost of practical AWH systems (*i.e.*, systems that condense water resulting in irreversibilities) to see if they can reach cost parity with existing desalination systems. Three different AWH systems are analyzed: active cooling (*i.e.*, a vapor compression refrigeration system that cools the air below the dew point to condense water), a passive radiative cooling surface (that radiates heat to space, reaching sub-ambient temperatures to condense water), and a sorbent with ambient cooling (that increases the humidity of the air through desorption and then condenses water when cooled to ambient temperature, which uses location and time specific weather data). Each of the AWH technologies requires water storage because water production varies with the fluctuating ambient humidity and temperature, while water demand is assumed to be constant. A levelized cost of water (LCOW) framework[15] is used to capture the capital and operating expenditures (including the cost of energy required) for each system. To find the LCOW of AWH systems in $/m³, Eq. (2) is used:

$$LCOW = \frac{(CAPEX_i + CAPEX_{WS} \times V_{WS,i}) \times (CRF)}{Yield_i} + OPEX_{fix} + OPEX_{e,i} \qquad (2)$$

where $CAPEX_i$ is the capital expenditure of the particular technology (in $ per unit system size), $CAPEX_{WS}$ is the capital expenditure of water storage (in $/m³ of water storage), $V_{WS,i}$ is the volume of water storage needed for a given AWH technology (in m³ of water storage per unit system size), CRF is the capital recovery factor which is equivalent to an amortization factor, $OPEX_{fix}$ accounts for fixed operations and maintenance costs (in in $ per unit system size per year), $Yield_i$ is the annual yield of water (in m³ of water per unit system size per year), and $OPEX_e$ is the variable operating costs associated with energy consumption (in $/m³ water). The subscript *i* in Eq. (2) corresponds to a particular technology being analyzed (either active cooling, passive cooling, or

sorbent). The system size is measured in tons of refrigeration for active cooling, m^2 of radiative cooling surface (TPX polymethylpentene sheet is assumed) for passive cooling, and kg of sorbent (MOF-303 is assumed[23,26]) for the sorbent system. All the input cost values and other assumptions for this model are given in Supplementary Note 1.

The $OPEX_e$ term can be calculated as the product of the energy cost (levelized cost of electricity or $LCOE$ in \$/kWh for active cooling, or heat $LCOH$ in \$/kWh_{th} for the sorbent system) and the specific energy consumption (SEC in kWh/m^3 of water for active cooling and kWh_{th}/m^3 of water for the sorbent system). We note that while sorbent AWH systems in the literature utilize "low-grade" heat sources such as solar or waste heat[19,22,24], this energy is not free since a solar collector/absorber (capital expenditure) is required to gather diffuse sunlight and transfer it to the sorbent using a heat exchanger. As such, even waste and solar heat have a non-zero $LCOH$ that must be considered[15,31,32]. Since energy costs vary widely with location, we also perform a sensitivity analysis to understand how this impacts the LCOW (Supplementary Note 5). The passive cooling system has no energy cost as the cooling surface is incorporated into the capital expenditure term, and we neglect the energy consumption of any fans required to blow air over the surface. Using this framework and Eq. (2), the specific energy required (SEC_i) to produce water with the three different practical AWH technologies (Supplementary Notes 6-8) was determined for three representative locations: Aruba (humid), Niger (dry), and Perth (highly variable humidity). The total LCOW and the cost breakdown for each system is shown in Fig. 4.
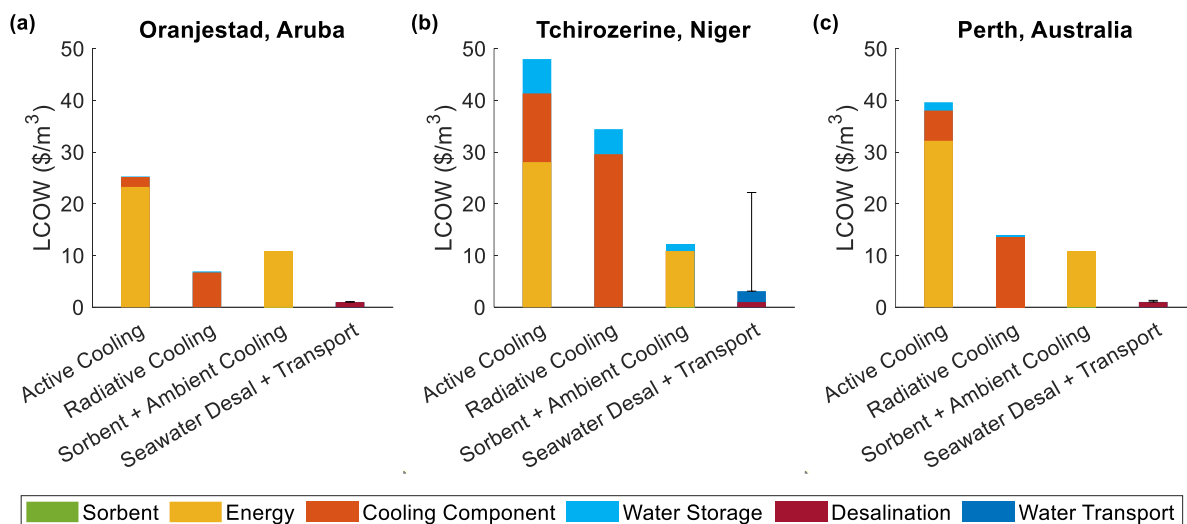
Fig. 4 | Comparison of practical AWH technologies. The LCOW of different AWH technologies (with practical, irreversible operation detailed in Supplementary Notes 6 – 8) in **(a)** Aruba, which has consistently high humidity; **(b)** Niger, which has consistently low humidity; **(c)** Perth, which has highly variable humidity throughout the year. The cooling component is a vapor compression system for active cooling, an ideal radiative cooling surface for passive cooling, and a metal condensing surface for the sorbent (MOF-303) with ambient cooling. The energy consumption is electricity (LCOE) for active cooling and heat (LCOH) for the sorbent. Even though these LCOW values were calculated for practical operation, some favorable assumptions were made (see Supplementary Notes 1, 6 – 8). For seawater desalination (reverse osmosis) with transport, the error bars correspond to 10× water transport costs (see Methods and Supplementary Note 1).

We find that the active cooling system is hindered by the large amount of energy required to condense water, resulting in very high LCOW values ($> \$20/m^3$), even in the humid location as shown in Fig. 4a. For the passive (radiative cooling) system on the other hand, the large surface area required to produce one m^3 of water drives up the cost, but it is less expensive than the active system in all three locations. The passive cooling system is also the cheapest option in very humid locations (represented by Aruba in this analysis) because it benefits from a high dew point while the sorbent system receives no benefits from an ambient humidity higher than the inflection point on the sorption isotherm (Supplementary Note 8). In arid regions as well as locations with highly variable humidity shown in Fig. 4b and 4c, the sorbent system has the lowest LCOW among AWH systems, which can be attributed to three main reasons. First, it is capable of absorbing moisture from as low as 13% relative humidity (while the active and passive cooling systems are not always

able to cool below the dew point without freezing the water). Second, the desorption process uses heat, which is significantly less expensive than electricity (making sorbents more suitable over the active cooling AWH systems). Third, the sorbent (MOF-303) and metal plate required to condense liquid water are inexpensive (see Supplementary Notes 1 and 8, respectively), resulting in the LCOW of the sorbent-based AWH system being dominated by the heat input alone. Even though this heat is inexpensive, a large amount of it is required (~1000 kWh_{th}/m^3 in all three locations), resulting in the LCOW ranging from $10 - 12$ \$/m^3 for sorbent AWH. For most cases the water storage cost is low, except when AWH is unable to produce water for a significant portion of the year. This happens when the air is too dry, preventing the cooling system from condensing water and the sorbent system from absorbing water. In addition, we considered a range of cutoff relative humidities below which the AWH system is not operated – this prevents the system from operating inefficiently (thus, reducing energy costs), but it also decreases the capacity factor (thus, increasing water storage costs). For each location, the cutoff relative humidity was calculated such that it minimizes the LCOW for each technology by balancing the energy and water storage costs.

In all cases, the AWH systems are more expensive than seawater desalination which has an LCOW of around $1/m^3 at the coast (based on operational reverse osmosis systems)[33,34]. In Fig. 4 we also calculate the cost of desalinating seawater at the nearest coast (using MATLAB's built-in Global Self-Consistent Hierarchical High-Resolution Geography data) and transporting the freshwater inland, allowing AWH and desalination to be directly compared for a given location. The water transportation cost is levelized over the lifetime of the transport infrastructure, which includes both capital and operating expenditures with values provided by Zhou and Tol[10] for a combination of pipes, canals, and tunnels (Methods). Given that literature data on water conveyance costs is very limited and may vary significantly, we analyze an additional scenario

where these transport costs (both horizontal and vertical) are increased by an order of magnitude to understand its effect on LCOW. When these higher water transport costs are considered (error bars in Fig. 4), we find that the LCOW of sorbent-based AWH in the Sahara Desert (representative arid location) can be lower than seawater desalination with transport (Fig. 4b). This appears to be the niche that sorbent AWH can fill cost-effectively: water production in very remote and dry locations, where no inland saline water source is available and water transport costs from the nearest coast are at least 5× higher than the values assumed here (Methods and Supplementary Note 3).

To understand exactly where sorbent AWH is optimal, we constructed Fig. 5, which shows a contour plot of the LCOW of coastal desalination with transport (Fig. 5a) and practical sorbent AWH (Fig. 5b). The map is only colored in locations where each particular technology is cheaper, and water transport costs of 5× the baseline value were considered. Fig. 5b reveals that the LCOW of AWH is relatively insensitive to location (owing to the low sorbent cost that we considered) and ranges from \$10.84/m^3 to \$12.76/m^3. The land area where sorbent AWH is cheaper corresponds to 6% of the WRW population. It should be noted that these results are highly sensitive to the transport costs. As such, in Supplementary Note 10 we present the results for the case when the transport cost is equal to the base value (sorbent AWH is cheaper for 0% of the WRW population) and the case when the transport cost is 10× the base value (sorbent AWH is cheaper for 32% of the WRW population).
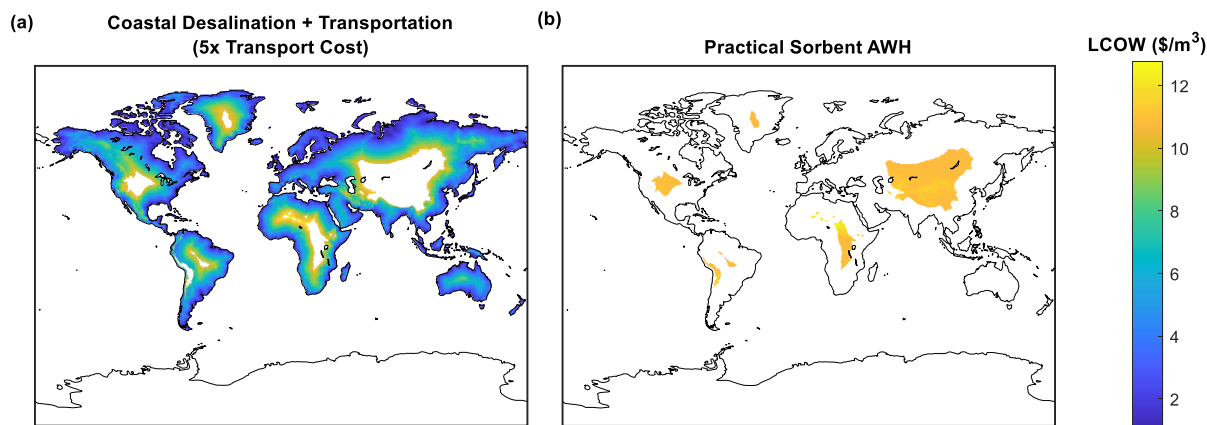
Fig. 5 | Maps of LCOW for desalination and sorbent AWH. Contour plot of the LCOW of coastal desalination with transport (a) and practical sorbent AWH (b). For this figure, a water transport cost 5× the base value was used (see Methods and Supplementary Note 1 for the base value). The map in (a) is colored only in locations where coastal desalination with transport is cheaper, while the map in (b) is colored in locations where sorbent AWH is cheaper.

To understand the absolute minimum LCOW that AWH systems can achieve by improving energy efficiency alone, we consider a hypothetical scenario in which the AWH can operate reversibly, thereby producing significantly more water for the same size (refrigeration tonnage, radiative cooling area, or sorbent mass) and energy input without incurring any increase in capital expenditure. We again optimized the cutoff relative humidity and maximum hourly water yield to find the lowest LCOW for AWH in each location. The results are shown in **Error! Reference source not found.** in terms of the ratio of the LCOW of reversible AWH to the LCOW of practical desalination with transport in all global locations. When this ratio is less than unity (green shaded region), reversible AWH is more cost effective than practical seawater desalination with transport; when the ratio is greater than unity (red shaded region), reversible AWH is more expensive. We find that reversible sorbent AWH would be cheaper than desalination for ~95% of the global WRW population, but reversible active and passive cooling AWH are cheaper for only ~33% and 5% of the global WRW population, respectively. While these reversible AWH costs are highly impractical, they reveal the best-case scenario for the different AWH technologies by increasing energy efficiency alone.
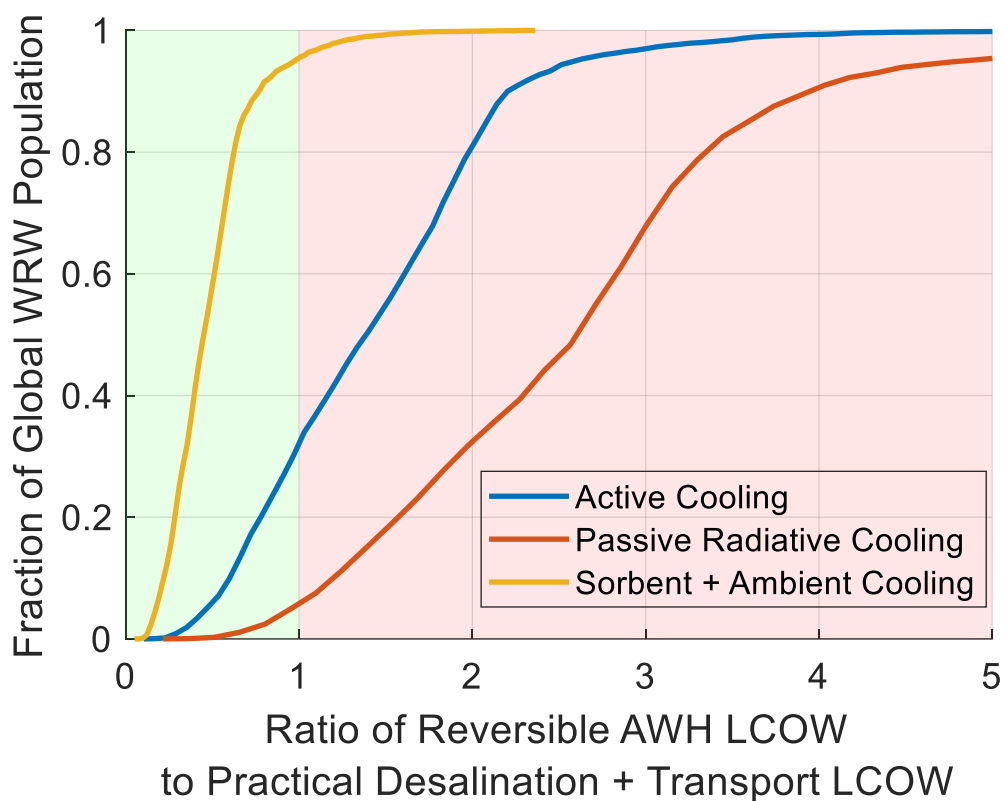
Fig. 6 | Levelized cost comparison of reversible AWH technologies to distributed desalination. Cumulative distribution of the ratio of the levelized cost of water of reversible atmospheric water harvesting to the levelized cost of water of practical desalination with transportation, for three different AWH systems. The value on the vertical axis corresponds to the fraction of the global water risk weighted (WRW) population that would have a ratio equal to or less than the value on the horizontal axis.

Opportunities for cost reduction in sorption-based AWH

The analysis thus far has shown that sorption-based systems are most viable among other AWH technologies. However, in order drive down the LCOW to become competitive with desalination, these systems must operate close to the reversible limit. This can be achieved with a system design that recuperates latent heat (*i.e.,* multi-stage operation[24]), but it would incur a significant cost increase due to the heat exchangers required for the multi-stage operation. Furthermore, increasing the number of stages beyond a certain point has diminishing returns, yielding only a small increase in efficiency for a sizeable increase in cost. Another, more realistic approach to reduce the LCOW is by using a low-cost heat source (*i.e.,* lower LCOH). In our

analysis of the practical sorbent AWH system, we used a regeneration temperature of 135 °C, as this results in the lowest specific energy consumption for a single-stage sorbent AWH system[26]. However, at a regeneration temperature of 80 °C, the SEC is only 37% higher, indicating that there is likely an optimal regeneration temperature that balances the cost of heat (which tends to increase with temperature[31,35]) with the energy consumption for desorption (which tends to decrease with temperature till the optimal regeneration temperature is reached). We discuss this further in Supplementary Note 5, where we perform a sensitivity analysis of the LCOH value and regeneration temperature – even a significant decrease in LCOH to 0.1 ¢/kWh would only result in LCOW values of $2.93/m³ and $2.53/m³ at regeneration temperatures of 80 °C and 135 °C, respectively; this approaches cost parity with desalination plus transport to a remote location. It is worth noting that the specific energy consumption increases rapidly as the regeneration temperature decreases below 80 °C[26], suggesting that the integration of lower temperature heat sources is not a worthwhile pursuit.

The technoeconomic analysis can also provide insight into the material properties that can contribute to lowering the LCOW. For example, a low specific heat for the sorbent is desirable, as a high specific heat increases the energy consumption beyond that of the reversible limit. The sorption isotherm inflection point should also be selected based on the climate of the location where the AWH system will be used. Specifically, this inflection point should correspond to a value near the lowest relative humidity experienced during the year, as this increases the number of hours when the sorbent can absorb moisture from air. However, the inflection relative humidity should not be too low, as this increases the specific energy consumption. For example, in Aruba, (the representative high humidity location), the relative humidity never dips below 43%, so the isotherm inflection point should not be close to this value. Overall, a careful balance of the capacity

factor (fraction of the year during which the sorbent can absorb moisture), energy consumption, and sorption kinetics is required to optimize the sorption isotherm for a particular location (beyond the scope of this work). While we only considered the desorption enthalpy of MOF-303 in our analysis (Methods), Li *et al.*[26] showed that the desorption enthalpy also affects the energy consumption of single-stage sorbent-based AWH (the energy consumption in a dual-stage sorbent AWH system decreased by nearly 40% when the desorption enthalpy changed from 2900 kJ/kg for MOF-303, to 3500 kJ/kg as the optimal value). Since our analysis shows that the energy consumption is the main cost driver for sorbent systems (assuming the sorbent material itself is inexpensive), optimizing the desorption enthalpy will likely play an important role in minimizing LCOW in sorbent systems. It is worth noting, however, that even with the optimal desorption enthalpy, the system considered by Li *et al.* would still have an LCOW greater than $6/m^3 owing to the energy consumption for desorption alone. The final parameter of interest is the cost of the sorbent (in $ per kg sorbent) divided by the water uptake of the sorbent (in kg water per kg sorbent). We find that if this value is less than $8.70 per kg water, the sorbent capital cost contributes less than $0.1/m^3 to the LCOW (see Supplementary Note 2) – this is the cost target that we establish for MOFs and other sorbents.

Finally, we note that while the optimization of all of these material properties is important, it would not be sufficient for sorbent-based AWH to reach cost parity with seawater desalination. This would require commensurate reductions in the system energy consumption and/or lower costs of heat as we discussed previously. Inland desalination (of nontraditional sources beyond seawater) should also be considered as an alternative method of distributed desalination, which will be discussed in a future manuscript.

Conclusions

This study presents the first comprehensive comparison of different AWH systems with desalination on the basis of both energy consumption (thermodynamic analysis) and cost (technoeconomic analysis). The key findings are:

- The median global water activity of atmospheric air (*i.e.*, relative humidity) is 0.65, whereas the activity of seawater is 0.97 owing to which reversible AWH would require over 10× higher energy consumption compared to reversible desalination.

- Even practical (irreversible) coastal seawater desalination with transport of this clean water to inland locations is more energy-efficient than reversible AWH for almost 90% of the global water risk-weighted population. Practical AWH systems would require significantly more energy owing to the enthalpy of condensation to produce liquid water, which is significantly higher than the reversible energy requirement (667 kWh_{th}/m^3 for condensation vs. 14 kWh/m^3 for reversible separation at a relative humidity of 70%).

- Evaluation of the AWH costs on a levelized basis shows that passive radiative cooling systems achieve the lowest LCOW among the AWH systems in humid locations, but this cost is still approximately 6× higher than the cost of seawater desalination (reverse osmosis) with transportation.

- In locations that are dry or have highly variable humidity, sorbent-based AWH systems achieve lower LCOWs than the active and passive cooling systems, but this cost of ~$11/m^3$ is still 3.53× higher than the cost of seawater desalination (reverse osmosis) with transportation in Niger.

- The niche that sorbent-based AWH can fulfill is when water conveyance costs are high and the location is far from the coast (*e.g.,* Sahara Desert). Furthermore, reversible operation is

unrealistic as the reduction in energy consumption would require large and thus expensive surfaces for heat and mass transfer.

- Material and system-level design modifications are required for sorbent-based AWH to approach cost parity with desalination. Specifically, the cost of heat ($LCOH$) would have to decrease by at least an order of magnitude to 0.1¢/kWh to approach the LCOW of seawater desalination with transport, assuming that the sorbent material itself costs less than $8.70 per kg water.

Overall, our analysis demonstrates that desalination is the preferred technology option for global freshwater production from an energy as well as cost standpoint.

Methods

Average Annual Relative Humidity

For the thermodynamic analysis, the average annual relative humidity for each location across the globe was calculated to estimate the average energy input accurately. For this, we used relative humidity data from NASA's MERRA 2 dataset[27] (which contains relative humidity data for each hour of the year in grid cells that span the globe). Because the least work of separation expression contains the natural logarithm of relative humidity, it is important to calculate the geometric mean of relative humidity, not the arithmetic mean. Then, the yearly geometric mean relative humidity and arithmetic mean temperature can be used to find the average annual least work of separation for a given location. It should be noted that using the geometric mean relative humidity and arithmetic mean temperature is an approximation, but it produces results with minimal error while significantly reducing computational time.

Weather, Population, and Water Risk Data

For weather (temperature and humidity) data, we used NASA's MERRA 2 dataset[27], which provides hourly temperature and humidity data within a 722×362 grid of the Earth's surface. This dataset was used for the thermodynamic analyses (Fig. 2 and Fig. 3) and cost analyses (Fig. 4, Fig. 5, and Fig. 6). We weighted our results by two factors: population density and the product of population with water risk. For this, gridded datasets for population[36] and water risk[37] were obtained to find the population and water risk within each cell of the 722×362 grid. For the specific locations analyzed in Fig. 4, TMYx data[38] was used.

Water Transportation Costs

For water transportation costs, we reference the work by Zhou and Tol[10], who performed a review of vertical and horizontal water transportation costs from various literature sources. They show a cost of $\$5 \times 10^{-4}$ per m^3 water per m of vertical distance transported, and we use this vertical transport cost in our analysis. They also provide a cost of $\$6 \times 10^{-4}$ per m^3 water per km of horizontal distance transported, which they state corresponds to canals, tunnels (108% more expensive than canals), and pipes (which are 271% more expensive than canals). Using this information, we assume an equal mix of canals, tunnels, and pipes, which results in a cost of $\$13.58 \times 10^{-4}$ per m^3 water per km of horizontal distance transported. It should be noted that using a mix of canals, tunnels, and pipes is common as evidenced by the Colorado River Aqueduct[39]. These horizontal and vertical costs were also increased by an order of magnitude to understand its impact on LCOW ($\$5 \times 10^{-3}$ per m^3 water per m of vertical distance and $\$13.58 \times 10^{-3}$ per m^3 water per km of horizontal distance for the high-cost scenario).

Data availability

The data that support the findings of this study are available in the Supplementary Information. Additional data are available from the corresponding author on request.

Acknowledgements

References

1. The Global Risks Report 2018.

2. Ritchie, H. & Roser, M. Water Use and Stress. *Our World in Data* (2017).

3. Water Scarcity. *UN-Water* https://www.unwater.org/water-facts/water-scarcity.

4. Vörösmarty, C. J. *et al.* Global threats to human water security and river biodiversity. *Nature* **467**, 555–561 (2010).

5. Lim, Y. J., Goh, K., Kurihara, M. & Wang, R. Seawater desalination by reverse osmosis: Current development and future challenges in membrane fabrication – A review. *Journal of Membrane Science* **629**, 119292 (2021).

6. Elimelech, M. & Phillip, W. A. The Future of Seawater Desalination: Energy, Technology, and the Environment. *Science* **333**, 712–717 (2011).

7. Jones, E., Qadir, M., van Vliet, M. T. H., Smakhtin, V. & Kang, S. The state of desalination and brine production: A global outlook. *Science of The Total Environment* **657**, 1343–1356 (2019).

8. Factsheet: People and Oceans. *United Nations* https://www.un.org/sustainabledevelopment/wp-content/uploads/2017/05/Ocean-fact-sheet-package.pdf (2017).

9. Mauter, M. S. & Fiske, P. S. Desalination for a circular water economy. *Energy Environ. Sci.* **13**, 3180–3184 (2020).

10. Zhou, Y. & Tol, R. S. J. Evaluating the costs of desalination and water transport. *Water Resources Research* **41**, (2005).

11. Foo, Z. H. *et al.* Solvent-driven aqueous separations for hypersaline brine concentration and resource recovery. *Trends in Chemistry* **4**, 1078–1093 (2022).

12. Finnerty, C. T. K. *et al.* Interfacial Solar Evaporation by a 3D Graphene Oxide Stalk for Highly Concentrated Brine Treatment. *Environ. Sci. Technol.* **55**, 15435–15445 (2021).

13. Haddad, A. Z. *et al.* Solar Desalination Using Thermally Responsive Ionic Liquids Regenerated with a Photonic Heater. *Environ. Sci. Technol.* **55**, 3260–3269 (2021).

14. Menon, A. K., Haechler, I., Kaur, S., Lubner, S. & Prasher, R. S. Enhanced solar evaporation using a photo-thermal umbrella for wastewater management. *Nat Sustain* **3**, 144–151 (2020).

15. Menon, A. K., Jia, M., Kaur, S., Dames, C. & Prasher, R. S. Distributed desalination using solar energy: A technoeconomic framework to decarbonize nontraditional water treatment. *iScience* **26**, 105966 (2023).

16. Chen, G. Thermodynamics of hydrogels for applications in atmospheric water harvesting, evaporation, and desalination. *Phys. Chem. Chem. Phys.* **24**, 12329–12345 (2022).

17. Rao, A. K., Fix, A. J., Yang, Y. C. & Warsinger, D. M. Thermodynamic limits of atmospheric water harvesting. *Energy Environ. Sci.* (2022) doi:10.1039/D2EE01071B.

18. Zhao, F. *et al.* Super Moisture-Absorbent Gels for All-Weather Atmospheric Water Harvesting. *Advanced Materials* **31**, 1806446 (2019).

19. Kim, H. *et al.* Adsorption-based atmospheric water harvesting device for arid climates. *Nat Commun* **9**, 1191 (2018).

20. Li, T. *et al.* Simultaneous atmospheric water production and 24-hour power generation enabled by moisture-induced energy harvesting. *Nat Commun* **13**, 6771 (2022).

21. Zhang, Y. *et al.* Atmospheric Water Harvesting by Large-Scale Radiative Cooling Cellulose-Based Fabric. *Nano Lett.* **22**, 2618–2626 (2022).

22. Lord, J. *et al.* Global potential for harvesting drinking water from air using solar energy. *Nature* **598**, 611–617 (2021).

23. Zheng, Z. *et al.* High-yield, green and scalable methods for producing MOF-303 for water harvesting from desert air. *Nat Protoc* 1–21 (2022) doi:10.1038/s41596-022-00756-w.

24. LaPotin, A. *et al.* Dual-Stage Atmospheric Water Harvesting Device for Scalable Solar-Driven Water Production. *Joule* **5**, 166–182 (2021).

25. Kwan, T. H., Yuan, S., Shen, Y. & Pei, G. Comparative meta-analysis of desalination and atmospheric water harvesting technologies based on the minimum energy of separation. *Energy Reports* **8**, 10072–10087 (2022).

26. Li, A. C. *et al.* Thermodynamic limits of atmospheric water harvesting with temperature-dependent adsorption. *Appl. Phys. Lett.* **121**, 164102 (2022).

27. MERRA-2 tavgM_2d_slv_Nx: 2d,Monthly mean,Time-Averaged,SIngle-level,Assimilation,Single-Level Diagnostics V5.12.4. *Goddard Earth Sciences Data and Information Services Center (GES DISC)* (2015).

28. Siegel, N. P. & Conser, B. A Techno-Economic Analysis of Solar-Driven Atmospheric Water Harvesting. *Journal of Energy Resources Technology* **143**, (2021).

29. Tu, R. & Hwang, Y. Performance analyses of a new system for water harvesting from moist air that combines multi-stage desiccant wheels and vapor compression cycles. *Energy Conversion and Management* **198**, 111811 (2019).

30. Haechler, I. *et al.* Exploiting radiative cooling for uninterrupted 24-hour water harvesting from the atmosphere. *Science Advances* **7**, eabf3978 (2021).

31. Gilbert, T., Menon, A. K., Dames, C. & Prasher, R. Heat source and application-dependent levelized cost of decarbonized heat. *Joule* **7**, 128–149 (2023).

32. Geffroy, C., Lilley, D., Parez, P. S. & Prasher, R. Techno-economic analysis of waste-heat conversion. *Joule* **5**, 3080–3096 (2021).

33. Baniasad Askari, I. & Ameri, M. A techno-economic review of multi effect desalination systems integrated with different solar thermal sources. *Applied Thermal Engineering* **185**, 116323 (2021).

34. Reimers, A. S. & Webber, M. E. Systems-level thermodynamic and economic analysis of a seawater reverse osmosis desalination plant integrated with a combined cycle power plant. *Texas Water Journal* **9**, 82–95 (2018).

35. Gabbrielli, R., Castrataro, P., Del Medico, F., Di Palo, M. & Lenzo, B. Levelized Cost of Heat for Linear Fresnel Concentrated Solar Systems. *Energy Procedia* **49**, 1340–1349 (2014).

36. Center For International Earth Science Information Network-CIESIN-Columbia University. Gridded Population of the World, Version 4 (GPWv4): Population Count, Revision 11. (2018) doi:10.7927/H4JW8BX5.

37. Aqueduct Water Risk Atlas. https://www.wri.org/applications/aqueduct/water-risk-atlas.

38. Repository of free climate data for building performance simulation. https://climate.onebuilding.org/.

39. MWD | Colorado River Aqueduct. *The Metropolitan Water District of Southern California* https://www.mwdh2o.com/colorado-river-aqueduct-map.